Terr. Atmos. Ocean. Sci., Vol. 28, No. 3, 217-228, June 2017 doi: 10.3319/TAO.2015.11.13.01(GSC)

A procedure for determining the preliminary maximum injection pressure for CO_2 sequestration

Der-Her Lee[1, 2], Cheng-Jie Liao[1], Jian-Hong Wu[1, 2, *], Yu-Fang Huang[1], and Guan-Lin Luo[1]

[1] *Department of Civil Engineering, National Cheng Kung University, Tainan City, Taiwan*
[2] *Sustainable Environment Research Center, National Cheng Kung University, Tainan City, Taiwan*

Article history:
Received 2 March 2012
Accepted 13 November 2015

Keywords:
Geological CO_2 storage, Failure criteria, In-situ stress, Maximum allowable injection pressure

Citation:
Lee, D.-H., C.-J. Liao, J.-H. Wu, Y.-F. Huang, and G.-L. Luo, 2017: A procedure for determining the preliminary maximum injection pressure for CO_2 sequestration. Terr. Atmos. Ocean. Sci., 28, 217-228, doi: 10.3319/TAO.2015.11.13.01(GSC)

ABSTRACT

Injection pressure applied in geological Carbon dioxide (CO_2) storage must exceed the existing pore pressure in the reservoir rock to sequestrate supercritical CO_2 underground. However, high injection pressure generates new fractures or re-activates existing faults in the rock mass, triggering seismic activities. Therefore, the maximum allowable reservoir rock injection pressure must be assessed as an essential parameter to secure CO_2 injection before proceeding with geological CO_2 storage. The failure criteria for saturated Yutengping Sandstone, which is a reservoir rock at Tiehchenshan, is investigated in this study using consolidated drained triaxial compression tests. The Mohr circles of in-situ stresses under different coefficients of critical fault friction and various depths are then drawn. The maximum allowable reservoir layer injection pressure was obtained through the relationship between the Mohr circles and failure criteria. The failure criterion for peak strength could be used in evaluating the generation of new fractures in intact rocks. The failure criterion for residual strength could be used in assessing the injection pressure causing slip on existing faults. This assessment method is therefore applicable in the preliminary analysis on the suitability and safety of a geological CO_2 storage site.

1. INTRODUCTION

Global warming has become a critical issue due to the recent global disasters caused by climate change. The increasing volume of greenhouse gas in the atmosphere is expected to accelerate global warming. Because Carbon dioxide (CO_2) is classified as a greenhouse gas, energy conservation, efficiency improvement, the use of low carbon energy (such as using renewable resources, nuclear and natural gas instead of coal to generate electricity), and Carbon Capture and Storage (CCS) are proposed approaches to reduce CO_2 emissions (Intergovernmental Panel on Climate Change (IPCC) 2005). Among these measures, CCS directly and efficiently reduces CO_2 emissions. The sequestration methods in CCS involve bio sequestration, mineralization, oceanic storage and geological storage.

Geological CO_2 storage injects supercritical CO_2 at high pressure through injection wells into depleted oil and gas reservoirs, coal mines or saline-water-saturated reservoir rocks. The injection pressure during supercritical CO_2 injection must therefore exceed the existing pore pressure in the reservoir rock to squeeze the existing fluids out and trap the supercritical CO_2 within the porous rock mass (Holloway and van der Straaten 1995). However, high injection pressure generates new fractures or reactivates existing faults in the rock mass, causing seismic activities. Supercritical CO_2 then leaks out along the new fractures and the reservoir seal is reduced, as shown by earlier studies (Rigg et al. 2001; Sminchak et al. 2002). Possible damage to the cap rocks caused by excessive CO_2 injection pressure could also lead to leakage. Therefore, the maximum allowable injection pressure must be assessed to avoid unexpected seismic activities and CO_2 leakage during CO_2 injections (Streit and Hills 2004).

The critical pressure and temperature of supercritical CO_2 is 7.38 MPa and 31.1°C, respectively. The reservoir rock must be deeper than 800 m (Bachu 2000). Rock at this depth withstands high confining pressure. Therefore, the maximum allowable reservoir rock injection pressure can be evaluated if the failure criteria and in-situ stresses of the reservoir rock can be determined. Wiprut and Zoback (2002),

* *Corresponding author*
E-mail: jhwu@mail.ncku.edu.tw

and Streit and Hills (2004) used the Mohr-Coulomb failure criterion to analyse the sliding potential for faults with different orientations and assessed the injection pressure that induces fault reactivation based on the in-situ stresses at storage sites and the relationship between the maximum horizontal principal stress and fault orientation. Rutqvist et al. (2007), Soltanzadeh and Hawkes (2009), and Cappa and Rutqvist (2011) used analytical and numerical simulations to assess the maximum allowable injection pressure and fault reactivation tendency during CO_2 sequestration, together with the rock deformation and permeability evolution during fault reactivation.

The failure criteria of the Yutengping Sandstone, which is the reservoir rock at Tiehchenshan, is investigated in this research by applying triaxial compressive tests under confining pressures. The existing pore pressure (P_f), vertical stress (S_v), minimum horizontal stress ($S_{h,\,min}$), and maximum horizontal stress ($S_{h,\,max}$) are calculated based on the stress gradient and the storage layer depth. The in-situ stress gradient of the Tiehchenshan structure against depth is obtained based on in-situ repeat formation tests, formation density log, and leak-off test results (Wang 2010). The maximum allowable injection pressure for Yutengping Sandstone is then obtained based on the relationship between the Mohr circle of in-situ stresses and the failure criteria. The proposed procedure can be used in preliminarily injection pressure evaluation during CO_2 sequestration through the injection well. However, more detailed assessment results obtained through numerical simulations are needed to understand more about the CO_2 sequestration effects on the storage layer mechanical properties.

2. ASSESSMENT OF MAXIMUM ALLOWABLE INJECTION PRESSURE

CO_2 injection into oil recovery or waste water pumping into deep rock formations have been carried out for decades. However, high injection pressure reactivates existing faults in the rock mass and causes seismic activities. For example, in 1962, a series of unusual earthquakes occurred shortly after waste water was injected into a rock formation at a depth of 12000 ft (3658 m) underground in the Rocky Mountain Arsenal in the United States (Nicholson and Wesson 1990). Sminchak et al. (2002) mentioned that supercritical CO_2 injection into reservoir rock caused the following phenomenon:

(1) Stress transfer to a weak fault zone,
(2) Hydraulic fracturing,
(3) Contraction of rocks due to the extraction of fluids,
(4) Subsidence due to the saturation of a rock formation,
(5) Mineral precipitation along a fault,
(6) Density-driven loadings.

The maximum allowable reservoir rock injection pressure is assessed to reduce the risk of seismic activities induced by CO_2 sequestration during the planning and design stages. The maximum allowable pressure highly depends on the in-situ stresses and failure criteria of the reservoir rock. In-situ stresses include pore pressure (P_f), vertical stress (S_v), minimum horizontal stress ($S_{h,\,min}$), and maximum horizontal stress ($S_{h,\,max}$) applied to the rock mass. The pore pressure increment is ΔP_f during CO_2 injection (Fig. 1a). Assume that the vertical and horizontal stresses are principal stresses. The original major principal stress of the reservoir rock mass before CO_2 injection is $\sigma_1 = S_{h,\,max} - P_f$. The minor principal stress is $\sigma_3 = S_{h,\,min} - P_f$. Additionally, assume that the porosity and permeability of the rock mass are large enough to distribute the pore pressure uniformly. The Mohr circle of the in-situ effective stress moves ΔP_f to the left and approaches the failure envelope (Fig. 1b). When the Mohr circle touches the failure envelope new fractures propagate or existing faults are reactivated in the rock mass. Therefore, the maximum allowable rock injection pressure can be calculated as the summation of ΔP_f, when the Mohr circle touches the failure envelop and the existing pore pressure is P_f in the rock mass.

The failure criteria can be established based on experimental data from triaxial compressive tests. Porous and weak sandstone is suitable as a reservoir rock. The sandstone

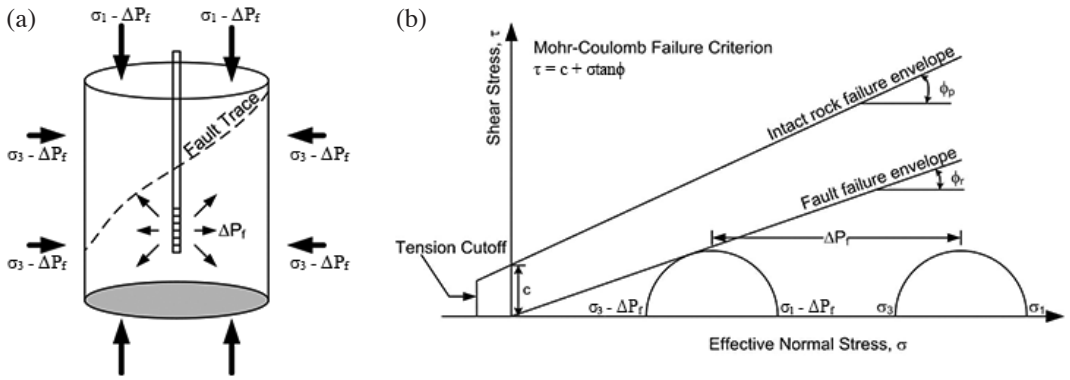

Fig. 1. Diagram illustrating how injection pressures reduce the effective stress of a rock formation.

strength is sensitive to the water content and confining pressure. Therefore, triaxial compressive tests are conducted on saturated sandstone samples with confining pressures similar to the in-situ stresses. The failure criteria can then accurately describe the rock strengths in the in-situ status.

3. RESEARCH METHOD

3.1 Site Selection

Fourteen potential sites including, Pate, Pingchen, Kengtzukou, Hukou-Yangmei, Chutung, Paoshan, Chuhuangken, Chinshui, Chingtsaohu-Chiting, Tiehchenshan, Paishatun, Yunghoshan, Pakuashan, and Niushan, are proposed for large scale geological CO_2 storage in Taiwan (Lu et al. 2008). The Tiehchenshan site potential capacity is roughly 320 million tons, which is the fourth largest among the sites. The Tiehchenshan site has been used as gas field to produce and store natural gas since the 1990s. Numerous relevant tests and geological data are available. The Tiehchenshan site was therefore selected as the research site in this study.

The caprock of the Tiehchenshan structure for the CO_2 storage consists of Chinshui and Shihliufen Shale. The storage layer consists of Yutengping Sandstone, Kuantaoshan Sandstone and Shangfuchi Sandstone. The Yutengping Sandstone is located between 1495 and 1697 m below ground surface and is the shallowest reservoir rock at the Tiehchenshan site. This sandstone is confined by Chinshui and Shihliufen Shale. The operational cost for CO_2 sequestration at the Yutengping Sandstone site is lower than that for Kuantaoshan Sandstone and Shangfuchi Sandstone. Therefore, Yutengping Sandstone was selected to conduct physical and mechanical tests to establish the failure criteria.

3.2 Test Material

3.2.1 In-Situ Sampling and Specimen Preparation

Yutengping Sandstone was named by Lin (1954) as the uppermost division of the Kueichulin Formation. This rock formation consists of a sandstone unit with abundant shale interbeds. The fresh sandstone is grey to light grey, fine-grained, thick to medium-bedded, and generally forms rows of hogback ridges. It is impure, containing a considerable amount of muddy matrix and thin interbeds and sandstone and shale interlaminations. Some carbonaceous particles are dispersed in the sandstone. The total thickness of the Yutengping Sandstone ranges from 250 - 550 m (Ho 1988).

Yutengping Sandstone core specimens were taken from borehole drilling at a great depth that is unavailable at the Tiehchenshan site in the research stage. Therefore, blocks of Yutengping Sandstone were obtained from outcrops in this study. The sampling site is located at Gongguan Village [TWD97 coordinate of (237651, 2714724)] in Miaoli County, Taiwan (Fig. 2). The rock block was removed from the outcrop and shaped to the appropriate size, as shown in Fig. 3a. The rock block was then drilled to obtain cylindrical specimens (5 cm in diameter, 10 cm in height) (Fig. 3b) for laboratory triaxial compressive tests.

The mechanical and physical properties of the Pliocene Yutengping Sandstone are very sensitive to the water content because of the short diagenesis period. Therefore, high-pressure gas instead of water was used to flush out dust and cool down the bit during core drilling. The outcrop sandstone exhibits a mild to moderately weathered character. The physical and mechanical properties of the samples are different from that of fresh sandstone taken from great depth. The strength of the sandstone may be underestimated from the outcrop specimen test results. This research is focused on the process for assessing allowable injection pressure using triaxial compressive and in-situ testing to secure geological CO_2 storage. The accurate allowable storage layer injection pressure can be assessed based on the same approach if fresh rock cores from the reservoir layer can be obtained from the in-situ borehole drilling.

3.2.2 Index Properties

Physical property, permeability and uniaxial compressive testing was conducted to obtain the index properties of the Yutengping Sandstone. The cylindrical specimen shown in Fig. 3b was air-dried, weighted and measured to obtain the Yutengping Sandstone dry unit weight, which is 20.23 kN m^{-3}. Huang (2011) pointed out that the Slake Durability index of Yutengping Sandstone, Id_2 = 7.63%, is considered very low in durability. A specific gravity test was applied to disintegrated Yutengping Sandstone grains soaked to obtain its specific gravity, which is about 2.61. The grains were also analysed using sieve and hydrometer analysis to obtain the grain size distribution curve, as shown in Fig. 4. This sand is classified as poor grade sand (SP) based on the Unified Soil Classification System (USCS). The unit weight, specific gravity obtained above and unit weight of water were then substituted into Eq. (1) to obtain the porosity n = 21%, which is suitable as geological CO_2 storage reservoir rock.

$$\gamma_d = (1 - n) G_s \gamma_w \quad (1)$$

In Pulse Velocity terms, the P- and S-wave of Yutengping Sandstone were measured according to the method suggested in ASTM D2845-08. The results obtained after the measurement of 75 specimens show that the average P-wave velocity of intact Yutengping Sandstone samples is 1536 m s^{-1}, and the average S-wave is 943 m s^{-1}. In permeability terms, the coefficient of permeability for Yutengping Sandstone was obtained using the triaxial permeability test.

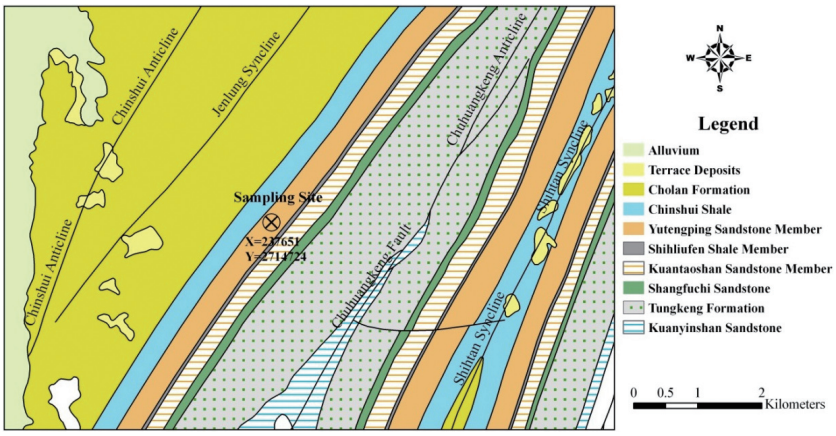

Fig. 2. Sampling site of Yutengping Sandstone. (Color online only)

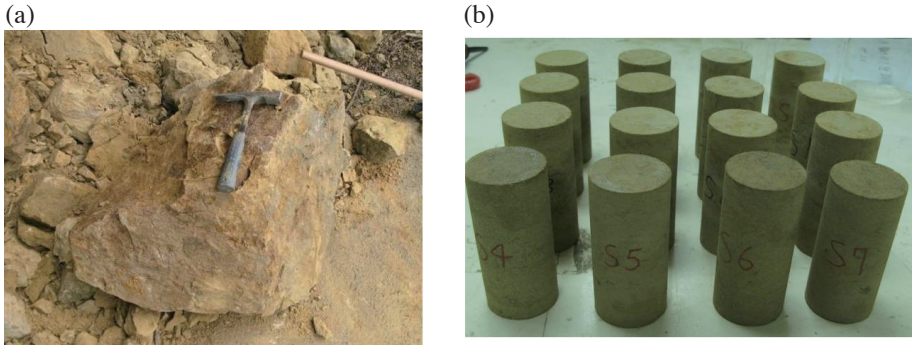

Fig. 3. (a) Rock taken from outcrop area (b) rock core specimens made by drilling. (Color online only)

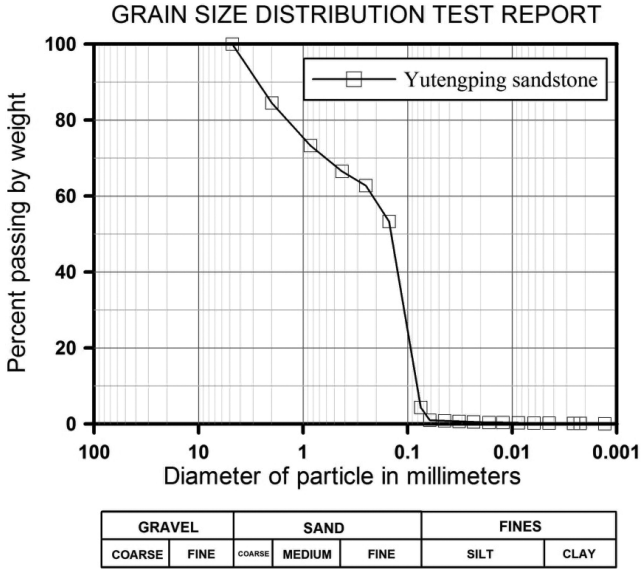

Fig. 4. Grain size distribution curve of Yutengping sandstone.

Specimen is enclosed in a thin rubber membrane within the triaxial chamber and a confining pressure σ_c = 0.8 MPa is applied. The pressure is set to 0.7 MPa at the inlet and 0.4 MPa at the outlet. Seepage discharge is then measured under the seepage pressure of 0.3 MPa. The coefficient of permeability for intact Yutengping Sandstone, $k = 4.84 \times 10^{-7}$ cm s^{-1}, is obtained in the end based on the relationship between the seepage discharge and time. Porosity and permeability considerably affect the injection rate in geological CO_2 storage. High injection pressure is needed to inject CO_2 into a reservoir rock with lower porosity and permeability and may reactivate the existing faults within the rock mass.

Three air-dried and saturated specimens were subjected to uniaxial compression tests using the displacement control method at a rate of 0.2 mm min^{-1}. The test results show that the uniaxial compressive strength of the air-dried specimen is $\sigma_{c,d}$ = 8.91 MPa but dropped to $\sigma_{c,s}$ = 4.31 MPa (decreases about 50%) for the saturated specimen. The uniaxial compressive strength of Yutengping Sandstone is sensitive to water content. The saturated specimens were used in triaxial compressive tests to establish the Yutengping Sandstone failure criteria. Table 1 lists the Yutengping Sandstone index properties.

3.3 Triaxial Compressive Tests

3.3.1 Test Apparatus

A suitable storage layer for CO_2 sequestration should be deeper than 800 m. At the Tiehchenshan site the depth of the interested reservoir rock, the Yutengping Sandstone, is 1500 m. A set of triaxial compressive test apparatus with maximum confining pressure up to 70 MPa was used to establish the failure criteria.

Figure 5 shows the apparatus including: (1) control system; (2) axial load unit; (3) confining pressure unit; and (4) triaxial cell. The control system includes a FlexTest GT controller and a PC. The FlexTest GT controller has a multi-tasking function that can simultaneously control 4 channels. Data measured by the sensors are transmitted back and recorded by the PC. The axial load unit consists of an actuator and a load frame. The actuator force is generated by hydraulic pressure and supported by the load frame as a counter-force. The confining pressure unit is a pressure intensifier (Fig. 5). Pressure is also generated by hydraulic pressure. The triaxial cell provides a confined space for the specimen. Deviator stress is applied to the rock samples through the axial rod until the specimen fails under specified confining pressure.

In the triaxial compressive test, the load cell measures the axial force applied to the rock sample. The LVDT monitors the axial displacement, and piezometers detect the confining pressure and back pressure. A volume burette measures the volume change in the rock sample. The load cell and LVDT capacities are 50 tons and ±100 mm, respectively. The maximum pressure for the pressure gauge is 70 MPa in measuring confining pressure and 10 MPa to detect back pressure.

3.3.2 Test Process

The specimen is placed in the triaxial cell that is encased by a thin rubber membrane to separate the rock sample from the confining fluid. Water is then filled into the cell and pressurized to a specified confining pressure. Hydraulic hoses are connected for confining pressure and back pressure, followed by load cell installation, LVDT, piezometers and other sensors. The data cable is connected to the controller.

The triaxial compressive test is divided into the following three stages: (1) the specimen is saturated, (2) the confining pressure is applied to the rock sample for consolidation, (3) the deviator stress is applied to the rocks. In Stage 1, 0.8 MPa of confining pressure and 0.7 MPa of back pressure are applied to the rock samples. The back pressure is applied to saturate the rock samples. The rock saturation is defined as the pore water pressure parameter, B, exceeds 90%. When the specimen is saturated Stage 2 initiates conducting different confining pressures (5, 10, 20, 40, and 60 MPa) to consolidate the Yutengping Sandstone samples with a load rate of 0.1 MPa min^{-1} under the undrained condition. The back pressure draining valve is then opened for rock consolidation. During consolidation the specimen is compressed and the pore water drains to the volume burette. At the end of consolidation Stage 3 starts by applying deviator stress to the specimen at a load rate of 0.2 mm min^{-1}. The draining valve remains open to measure the volume change in the specimen.

The deviator stress curve versus axial strain and volumetric strain curve versus axial strain in the triaxial compressive tests can be obtained to realize the shear behavior (dilation/contraction) of Yutengping Sandstone under different confining pressures. The failure criteria for the peak and residual Yutengping Sandstone strengths are then obtained.

4. EXPERIMENTAL RESULTS

Supercritical CO_2 is injected into a reservoir rock at great depth to sequestrate CO_2 underground. High injection pressure can generate new fractures or reactivate existing faults in the rock mass. Therefore, the maximum allowable injection pressure is a key factor to assure the safety of CO_2 sequestration. Triaxial compressive tests were conducted on Yutengping Sandstone, which is a reservoir rock at Tiehchenshan, to establish the failure criteria. The maximum allowable injection pressure for Yutengping Sandstone can be assessed based on the failure criteria and the in-situ stresses.

4.1 Results of Triaxial Compressive Tests

Figure 6 shows the deviator stress and volumetric

Table 1. Basic characters of Yutengping Sandstone.

Name	γ_d (kN m^{-3})	G_s	n (%)	USCS	V_p (m s^{-1})	V_s (m s^{-1})	k (cm sec^{-1})	$\sigma_{c,d}$ (MPa)	$\sigma_{c,s}$ (MPa)
Yutengpin Sandstone	20.23	2.61	21	SP	1536(273)	943(98)	4.84×10^{-7}	8.91	4.31

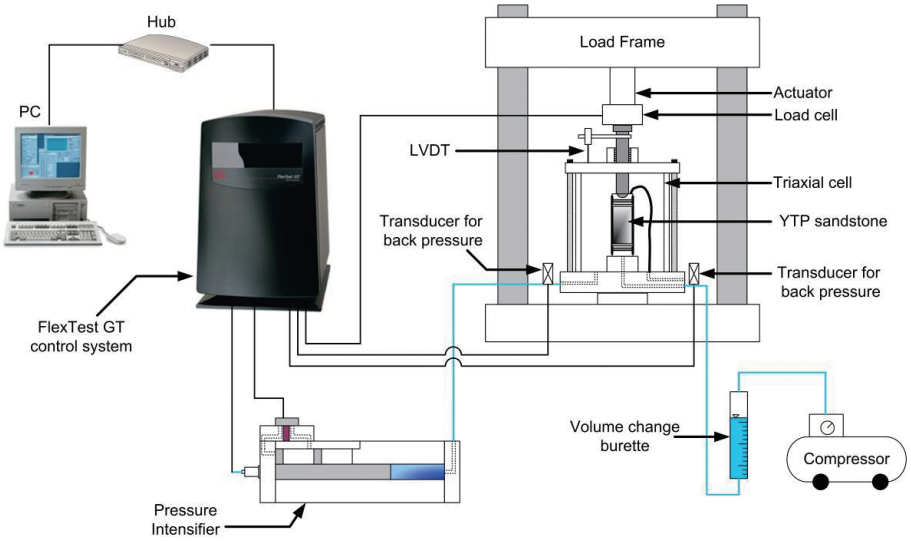

Fig. 5. Diagram illustrating triaxial compression test apparatus. (Color online only)

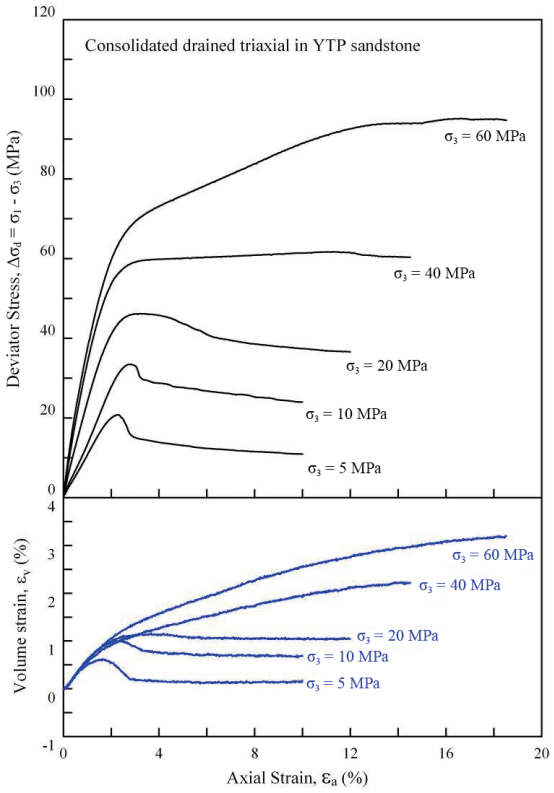

Fig. 6. Variation curves of deviator stress and volumetric strain in triaxial compression test. (Color online only)

strain curves in the triaxial compressive tests. The deviator stress applied to fail the sample increases as the confining pressure increases.

The brittle-ductile transition pressure of Yutengping Sandstone is about 40 MPa based on the stress-strain curves under different confining pressures. Figure 7a shows obvious failure surface in the rock sample in the brittle failure when the confining pressure is 5 MPa. Moreover, ductile failure occurred (Fig. 7b) as the confining pressure exceeds the brittle-ductile transition pressure.

Figure 6 shows the contractive volumetric strain turns into dilation before the deviator stress reaches its peak in the brittle failure, and the volumetric strain remains constant when the deviator stress reaches the residual state. In the ductile failure mode the volumetric strain increases continuously as the derivative stress increases. The confining pressure therefore dominates the strength and failure behavior of Yutengping Sandstone.

Table 2 lists the tangent modulus of elasticity [$E_{t(50\%)}$] and strength parameters of Yutengping Sandstone. Figure 8 shows a graph showing the tangent modulus of elasticity against the corresponding confining pressure in the semi-log coordinate system. The relationship between the tangent modulus of elasticity, $E_{t(50\%)}$, and the confining pressure, σ_3, is regressed as Eq. (2). The modulus of elasticity could be an input parameter for hydro-mechanical numerical simulations.

$$E_{t(50\%)} = 987.6 \log \sigma_3 + 426.8 \quad (2)$$

The Mohr circles of Yutengping Sandstone at peak strength are shown in Fig. 9a. The brittle failure envelope of Yutengping Sandstone is drawn as the tangent passing through the Mohr-Coulomb failure criteria with confining pressures of 5, 10, and 20 MPa. The peak shear strength parameters are $c_p = 4.41$ MPa and $\phi_p = 26.9°$ and the Mohr-Coulomb failure criterion can be written using Eq. (3):

$$\tau_p = 4.41\,(\text{MPa}) + \sigma \tan(26.9°) \quad (3)$$

Equation (3) is correct when the Yutengping Sandstone is in the brittle failure mode.

Meanwhile, Fig. 9b shows the Mohr circles of the Yutengping Sandstone for the residual strength drawn based on the stresses listed in Table 2. The residual shear strength parameters are $c_r = 1.95$ MPa and $\phi_r = 25.2°$. The Mohr-Coulomb failure criterion for the residual strength is represented by Eq. (4):

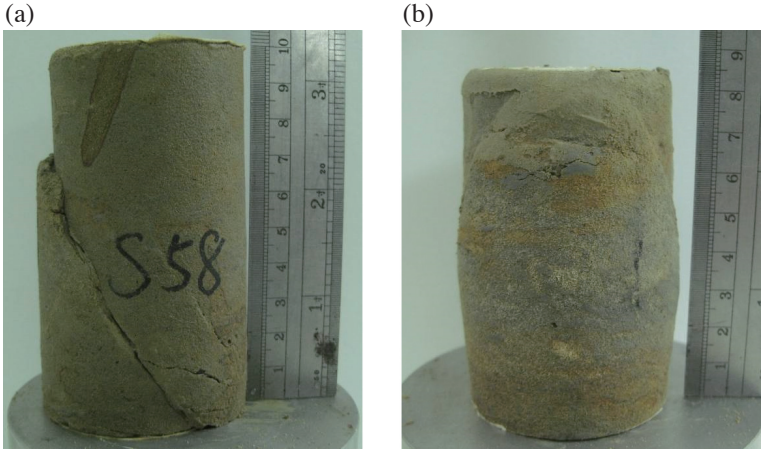

Fig. 7. The impact of different confining pressure amounts to specimen failure. (a) $\sigma_3 = 5$ MPa; (b) $\sigma_3 = 60$ MPa. (Color online only)

Table 2. Consolidated drained triaxial compression test results of saturated Yutengping Sandstone.

No	$E_{t(50\%)}$ (MPa)	σ_3 (MPa)	$\sigma_{1,p}$ (MPa)	$\sigma_{1,r}$ (MPa)	Mohr-Coulomb criterion			
					c_p (MPa)	ϕ_p (°)	c_r (MPa)	ϕ_r (°)
S-58	1105	5	25.6	15.8	4.41	26.9	1.95	25.2
S-57	1496	10	43.4	33.9				
S-56	1582	20	66.1	56.5				
S-52	1980	40	-*	100.9				
S-59	2245	60	-*	154.6				

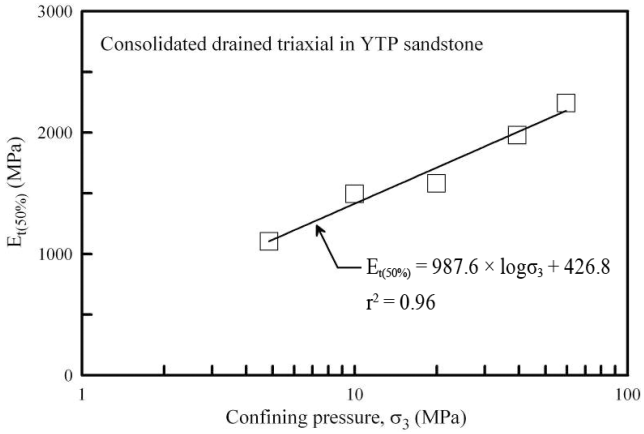

Fig. 8. The relationship between tangent modulus of elasticity and confining pressure for saturated Yutengping Sandstone.

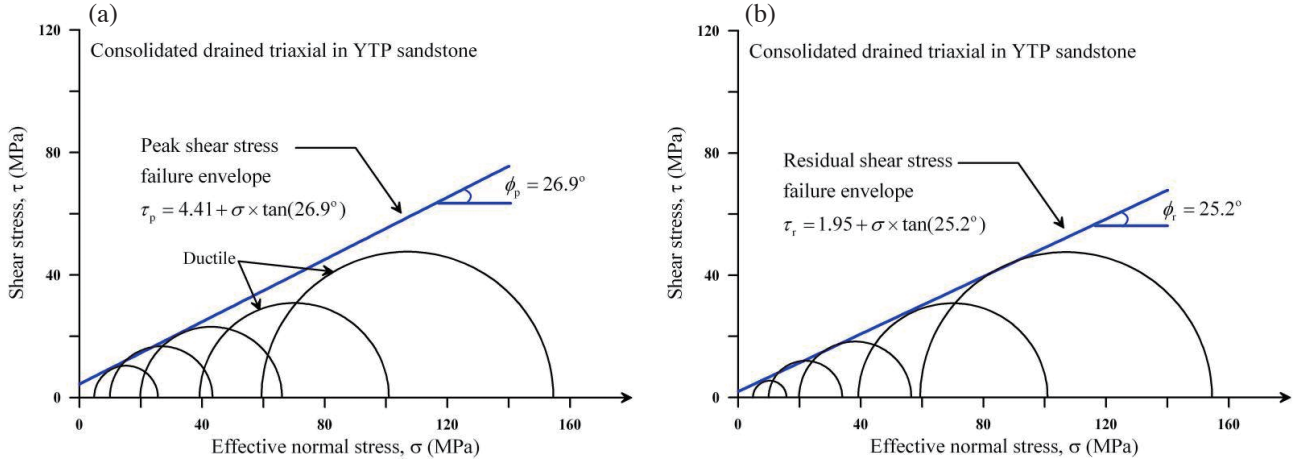

Fig. 9. Mohr circles from the results of triaxial compression test with their failure criteria. (a) Peak state; (b) residual state. (Color online only)

$$\tau_r = 1.95\,(\text{MPa}) + \sigma \tan(25.2°) \quad (4)$$

4.2 Maximum Allowable Injection Pressure

4.2.1 In-Situ Stress Assessment

Both in-situ stresses and failure criteria for Yutengping Sandstone are the essential parameters used to assess the maximum allowable injection pressure. The failure criteria can be established based on the peak and residual strengths of Yutengping Sandstone using triaxial compressive tests. The in-situ formation pore pressure stress (P_f), vertical stress (S_v), minimum horizontal stress ($S_{h,\,min}$), and maximum horizontal stress ($S_{h,\,max}$) can be evaluated from various in-situ tests.

At the Tiehchenshan site, Wang (2010) concluded that the vertical stress (S_v) was estimated from density log results. The minimum horizontal stress ($S_{h,\,min}$) was calculated based on leak-off and concrete extrusion tests. The in-situ pore pressure (P_f) was obtained using the repeat formation test. Figure 10 shows the variation in in-situ stresses against the depth (Wang 2010). The stress gradient $S_v = 23.60$ MPa km^{-1} and the minimum horizontal stress $S_{h,\,min} = 18.70$ MPa km^{-1}. The formation pore pressure gradient is 9.47 MPa km^{-1} at depths less than 3 km and is 14.24 MPa km^{-1} at depths greater than 3.4 km.

Hung et al. (2009) analyzed the well logging and leak-off test data from TCDP (Taiwan Chelungpu-fault Drilling Project) and discovered the in-situ stresses in Western Taiwan resulted in a strike-slip fault after the Chi-Chi earthquake in 1999. Therefore, the maximum horizontal stress ($S_{h,\,max}$) can be calculated using the following Eq. (5) based on the critical friction fault theory (Anderson 1951) if the minimum horizontal stress is known.

$$\frac{\sigma_1}{\sigma_3} = \frac{S_{h,\,max} - P_f}{S_{h,\,min} - P_f} = \left(\sqrt{1+\mu^2} + \mu\right)^2 \quad (5)$$

Where μ is the coefficient of critical friction of fault.

Byerlee (1978) suggested that the μ is between 0.6 and

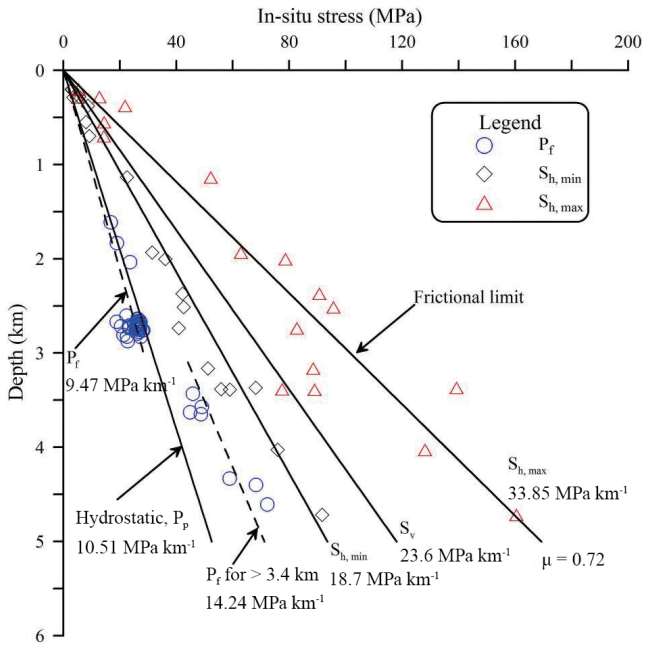

Fig. 10. The relationship between in-situ stresses and depth in Tiehchenshan site (μ = 0.72) (Wang 2010). (Color online only)

0.85. Therefore, the maximum horizontal stresses with μ = 0.6, 0.72, and 0.85 are calculated. In Fig. 10 (Wang 2010), the maximum horizontal stress gradient against depth is 33.85 MPa km^{-1} when the coefficient of friction is μ = 0.72. Similarly, the gradient is 29.91 and 38.91 MPa km^{-1} when μ = 0.6 and 0.85, respectively.

The vertical depth of Yutengping Sandstone at Tiehchenshan site starts from 1495 m at the top and 1697 m at the bottom (Lu et al. 2008). Therefore, the supercritical CO_2 must be injected to depths between 1495 and 1697 m underground when the Yutengping Sandstone is considered as the reservoir rock. Table 3 lists the calculated in-situ stresses at depths of 1495 and 1697 m. The maximum horizontal stress increases as the value of μ increases.

The in-situ stress accuracy can certainly be improved by the new core-based techniques, i.e., acoustic emission, deformation rate analysis (Wu and Jan 2010; Wu and Pan 2013) and elastic strain recovery method (Lin et al. 2007) if in-situ fresh cores drilled from great depth can be obtained.

4.2.2 Assessment Result

We assume that the horizontal and vertical stresses are principle stresses. The principal stresses at various depths and under critical fault coefficients of friction are calculated in Table 3. When the depth is 1495 m and μ = 0.72, the minor principal stress σ_3 is 13.8 MPa, intermediate principal stress σ_2 is 21.12 MPa, and the major principal stress σ_1 is 36.45 MPa (Table 4). From this we know that the confining pressure (minor principal stress) sustained by Yutengping Sandstone is 13.8 MPa, and its brittle-ductile transition pressure is 40 MPa. Consequently, brittle failure will occur under the current stress condition while the strength and allowable injection pressure at failure could be assessed through Eq. (3).

Injection pressure in geological CO_2 storage increases the existing pore pressure and decreases the effective stress in the rock mass. Therefore, the Mohr circle moves left toward the failure envelope. The Mohr circle movement, having the diameter of the difference between the in-situ major and minor principal stresses, is about 8.78 MPa to the left to touch the peak failure envelope of the Yutengping Sandstone (Fig. 11a). The maximum allowable injection pressure for a reservoir rock can be calculated by summing the $\Delta P_{f, peak}$ and the original pore pressure in the rock mass, P_f. Therefore, the maximum allowable injection pressure of the intact Yutengping Sandstone is 22.94 MPa at 1495 m depth underground and μ = 0.72.

If a fault exists in the Yutengping Sandstone, the failure criteria for the residual strength can be adopted for assessing the maximum allowable CO_2 injection pressure instead of the peak strength criteria. Figure 11b shows that when the fault orientation forms an angle of $q = 45° - \phi_r/2$ with the major principal stress, the $\Delta P_{f, residual}$ decreases to 2.66 MPa with the residual failure criteria. Wang (2010) determined the borehole breakout location based on four-arm caliper tools (HDT), and found that the maximum horizontal principal stress orientation ($S_{h, max}$) of Yutengping Sandstone was at N28°E. From this, it is known that the injection pressure will move the Mohr Circle tangent to the failure envelope and cause fault reactivation when the fault orientation is N4.4°W and N60.4°E. On the other hand, the injection

Table 3. Possible in-situ stresses of Yutengping Sandstone at different depth.

Depth (km)	P_f (MPa)	S_v (MPa)	$S_{h,min}$ (MPa)	$S_{h,max}$ (MPa)		
				μ = 0.6	μ = 0.72	μ = 0.85
1.495	14.16	35.28	27.96	44.72	50.61	58.17
1.697	16.07	40.05	31.73	50.76	57.44	66.03

Table 4. Principal stresses and the maximum allowable injection pressure increment amounts of Yutengping Sandstone under various conditions.

Depth (km)		1.495	1.697
$\sigma_3 = S_{h,min} - P_f$ (MPa)		13.80	15.66
$\sigma_2 = S_v - P_f$ (MPa)		21.12	23.98
μ = 0.6	$\sigma_1 = S_{h,max} - P_f$ (MPa)	30.56	34.69
	$\Delta P_{f,peak}$ (MPa)	12.36	12.85
	$\Delta P_{f,residual}$ (MPa)	6.65	6.99
μ = 0.72	$\sigma_1 = S_{h,max} - P_f$ (MPa)	36.45	41.37
	$\Delta P_{f,peak}$ (MPa)	8.78	8.79
	$\Delta P_{f,residual}$ (MPa)	2.66	2.46
μ = 0.85	$\sigma_1 = S_{h,max} - P_f$ (MPa)	44.01	49.96
	$\Delta P_{f,peak}$ (MPa)	4.22	3.62
	$\Delta P_{f,residual}$ (MPa)	-2.42 (N.G.)	-3.31 (N.G.)

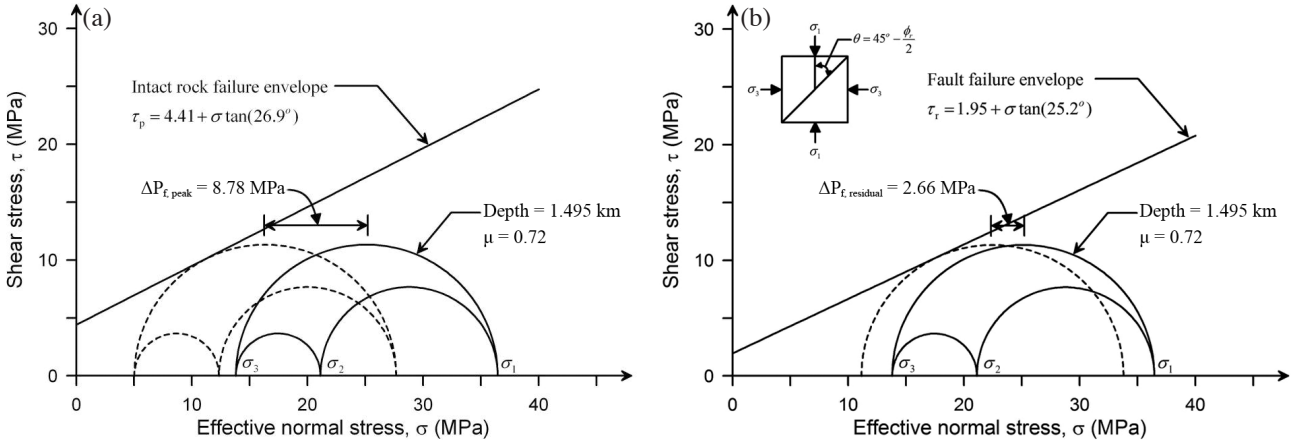

Fig. 11. Assessment result for the maximum allowable injection pressure increment amount (depth = 1.495 km, μ = 0.72).

pressure should be increased to match the major principal stress in order to cause fault reactivation when the fault orientation is perpendicular to the major principal stress. Thus, the fault orientation could affect the allowable injection pressure magnitude. Since the storage formation geological structure strongly governs the maximum allowable injection pressure, a conservative concept applying the residual strength to analyze the maximum allowable injection pressure is required when the properties and locations of local geological structures are indistinct. In Table 4 when μ = 0.85 the $\Delta P_{f,residual}$ assessed by the residual failure criterion state is negative, which indicates that the Yutengping Sandstone failed prior CO_2 injection. However, because the storage layer is currently stable before the geological CO_2 storage starts, the assumption of μ = 0.85 in the residual state is unreasonable. As the μ increases the maximum horizontal stress, $S_{h,max}$, and the diameter of the Mohr circle increases but the maximum allowable injection pressure decreases.

In summary, the Yutengping Sandstone blocks used in this research were obtained from an outcrop due to budgetary considerations. Thus, the degree of rock weathering will affect its strength, resulting in underestimation of the maximum allowable reservoir rock injection pressure. In addition, the assessment of maximum horizontal stress, $S_{h,\,max}$ was performed using theoretical equations under the assumption that the coefficients of critical fault friction lies between 0.6 and 0.85, which is not the actual value. Thus, the main purpose of this research is establishing a testing and assessment method. The maximum allowable injection pressure obtained in this research is provided just for reference. In practical applications the failure criteria should be established using core specimens obtained by drilling and in-situ tests should be conducted to measure parameters such as in-situ stresses and their orientation to improve results usability. In the end, the effects of different conditions and sequestration methods on the mechanical properties of the overall reservoir environment can be understood using numerical simulations.

5. CONCLUSION

Conclusions can be given as follows:

(1) The failure criteria of reservoir rocks were established in this research using triaxial tests and Mohr circles drawn according to the in-situ stresses. The maximum allowable injection pressure was assessed based on the relationship between the Mohr circles and the failure criteria. The proposed procedure is suitable for estimating the allowable injection pressure in geological CO_2 storage.

(2) The confining pressure sustained by the rocks is high since CO_2 sequestration is done at depths greater than 800 m. However, the injection of supercritical CO_2 decreases the effective stress in a rock mass, which could cause brittle failure. Therefore, the mechanical properties of reservoir rocks are very important. The mechanical behavior and strength properties of rocks under different confining pressures could be understood using the triaxial compressive test apparatus developed in this research. Regardless of the shear strength parameters the magnitude of brittle-ductile transition pressure, or the relationship between the modulus of elasticity and confining pressure, could all be used in numerical simulation analysis to obtain a more thorough understanding of the changes in mechanical properties in reservoir rocks during CO_2 sequestration.

(3) More studies are required to investigate the impact of temperature on the shear strength of the Yutengping Sandstone since the geothermal gradient and supercritical CO_2 control the reservoir rock temperature. Additionally, highly accurate maximum allowable injection pressure can be assessed if the failure criteria and in-situ stresses can be properly evaluated using in-situ fresh cores taken at great depth. Ground deformation and seismicity must be monitored to detect new fracturing and reactivation of existing faults in the rock mass.

Acknowledgements This paper is the research result of NSC 100-3113-E-008-002. Thanks to NSC, Taiwan for sponsoring this project.

REFERENCES

Anderson, E. M., 1951: The Dynamics of Faulting and Dyke Formation with Applications to Britain, Oliver and Boyd, Edinburgh, 206 pp.

Bachu, S., 2000: Sequestration of CO_2 in geological media: Criteria and approach for site selection in response to climate change. *Energ. Convers. Manage.*, **41**, 953-970, doi: 10.1016/S0196-8904(99)00149-1. [Link]

Byerlee, J., 1978: Friction of rocks. *Pure Appl. Geophys.*, **116**, 615-629, doi: 10.1007/BF00876528. [Link]

Cappa, F. and J. Rutqvist, 2011: Modeling of coupled deformation and permeability evolution during fault reactivation induced by deep underground injection of CO_2. *Int. J. Greenh. Gas Con.*, **5**, 336-346, doi: 10.1016/j.ijggc.2010.08.005. [Link]

Ho, C. S., 1988: An Introduction to the Geology of Taiwan Explanatory Text of the Geologic Map of Taiwan, Central Geological Survey of Taiwan, Taipei, 192 pp. (in Chinese)

Holloway, S. and R. ven der Straaten, 1995: The joule II project the underground disposal of carbon dioxide. *Energ. Convers. Manage.*, **36**, 519-522, doi: 10.1016/0196-8904(95)00057-K. [Link]

Huang, Y. F., 2011: Investigations of the injection pressure and mineral trapping improvement technologies for geological storage of CO_2: A case study of Tiehchenshan anticline. Master Thesis, Department of Civil Engineering, National Cheng Kung University, Tainan City, Taiwan, 118 pp. (in Chinese)

Hung, J. H., K. F. Ma, C. Y. Wang, H. Ito, W. Lin, and E. C. Yeh, 2009: Subsurface structure, physical properties, fault-zone characteristics and stress state in scientific drill holes of Taiwan Chelungpu Fault Drilling Project. *Tectonophysics*, **466**, 307-321, doi: 10.1016/j.tecto.2007.11.014. [Link]

Lin, C. C., 1954: Geology of Taiwan, in Taiwan Hsin-Chih, China Culture Publishing Foundation, Taipei City, Taiwan, 14-47. (in Chinese)

Lin, W., T. Hirono, E. C. Yeh, W. Tanikawa, and W. Soh, 2007: Core handling and real-time non-destructive characterization at the Kochi core center: an example of core analysis from the Chelungpu Fault. *Sci. Dril.*, 103-106, doi: 10.2204/iodp.sd.s01.35.2007. [Link]

Lu, M. T., T. H. Hsiuan, Y. J. Huang, and C. H. Fan, 2008:

Potential estimate of geological storage for CO_2 onshore Taiwan. *Mining Metallurgy*, **52**, 154-161. (in Chinese)

Nicholson, C. and R. L. Wesson, 1990: Earthquake hazard associated with deep well injection: A report to the U.S. environmental protection agency. Open-File Report, U.S. Geological Survey Bulletin, Washington, D.C., 74 pp.

Rigg, A., G. Allison, J. Bradshaw, J. Ennis-King., C. Gibson-Poole, R. Hillis, S. Lang, and J. Streit 2001: The search for sites for geological sequestration of CO_2 in Australia: A progress report on GEODISC. *APPEA J.*, **41**, 711-725.

Rutqvist, J., J. Birkholzer, F. Cappa, and C. F. Tsang, 2007: Estimating maximum sustainable injection pressure during geological sequestration of CO_2 using coupled fluid flow and geomechanical fault-slip analysis. *Energ. Convers. Manage.*, **48**, 1798-1807, doi: 10.1016/j.enconman.2007.01.021. [Link]

Sminchak, J., N. Gupta, C. Byrer, and P. Bergman, 2002: Issues related to seismic activity induced by the injection of CO_2 in deep saline aquifers. *J. Energy Environ. Res.*, **2**, 32-46.

Soltanzadeh, H. and C. D. Hawkes, 2009: Assessing fault reactivation tendency within and surrounding porous reservoirs during fluid production or injection. *Int. J. Rock Mech. Min. Sci.*, **46**, 1-7, doi: 10.1016/j.ijrmms.2008.03.008. [Link]

Streit, J. E. and R. R. Hills, 2004: Estimating fault stability and sustainable fluid pressures for underground storage of CO_2 in porous rock. *Energy*, **29**, 1445-1456, doi: 10.1016/j.energy.2004.03.078. [Link]

Wang, L. J., 2010: In-situ stress field and fault reactivation analysis in the Tienchanshan field, west-central Taiwan. Master Thesis, Graduate Institute of Applied Geology, National Central University, Taoyuan City, Taiwan, 81 pp. (in Chinese)

Wiprut, D. and M. D. Zoback, 2002: Fault reactivation, leakage potential, and hydrocarbon column heights in the northern North Sea. *Norwegian Pet. Soc. Spec. Publ.*, **11**, 203-219, doi: 10.1016/S0928-8937(02)80016-9. [Link]

Wu, J. H. and S. C. Jan, 2010: Experimental validation of core-based pre-stress evaluations in rock: A case study of Changchikeng sandstone in the Tseng-wen reservoir transbasin water tunnel. *Bull. Eng. Geol. Environ.*, **69**, 549-559, doi: 10.1007/s10064-010-0265-3. [Link]

Wu, J. H. and Y. W. Pan, 2013: Three-dimensional in situ stress evaluation using a new under-coring technique: The Tseng-Wen reservoir transbasin water tunnel. *Environ. Earth. Sci.*, **68**, 77-86, doi: 10.1007/s12665-012-1717-9. [Link]